Molecular modeling of the poling of piezoelectric polyimides

J.A. Young[a,*], B.L. Farmer[a], J.A. Hinkley[b]

[a]Department of Materials Science and Engineering, University of Virginia, Charlottesville, VA 22903, USA
[b]Materials Division, NASA Langley Research Center, Hampton, VA 23681, USA

Abstract

The computational method described in this paper allows the calculation of the dielectric relaxation strength of an amorphous polymer based solely upon its chemical structure. The 4,4′ oxydiphthalic anhydride (ODPA) dianhydride and bis-aminophenoxybenzene (APB) diamine based polyimides, (β-CN) APB–ODPA and APB–ODPA were studied. Amorphous cells were constructed and then poled using molecular dynamics. Dielectric relaxation strengths of $\Delta\epsilon = 17.8$ for (β-CN) APB–ODPA and $\Delta\epsilon = 7.7$ for APB–ODPA were predicted. These values are in excellent agreement with the experimental values. It was found that both the pendant nitrile dipole and the backbone anhydride residue dipole make significant contributions to the polyimides' dielectric response. Specifically, it was shown that the difference in the magnitude of the dielectric relaxations is directly attributable to the nitrile dipole. The size of the relaxations indicate an absence of cooperative dipolar motions. The model was used to explain these results in terms of the average orientation of the nitrile and anhydride dipoles to within 51° and 63°, respectively, of the applied electric field. © 1999 Elsevier Science Ltd. All rights reserved.

Keywords: Dielectric relaxation strength; Amorphous polymer; Piezoelectric polymers

1. Introduction

The goal of this work is to develop an understanding of the behaviour and properties of high temperature piezoelectric polymers. Since 1963, piezoelectric activity in polymers has been the subject of much scientific and economic interest [1,2]. The semicrystalline polymer polyvinylidene fluoride (PVDF) dominates recent literature [3]. Although PVDF shows a large piezoelectric response, it has a maximum use temperature of only 363 K [2]. Polyimides are of particular interest due to their high temperature stability and the ease with which various pendant groups may be placed upon them. Molecular modeling can provide a fundamental understanding of the polyimide's response to temperature and applied electric field. Computational chemistry techniques, including both quantum and classical mechanics, have been used to predict and understand the piezoelectric response of amorphous polyimides.

Piezoelectricity arises from the coupling between elastic variables [stress (X) or strain (x)] and dielectric variables [electric displacement (D) or electric field (E)]. To produce a piezoelectric material from an amorphous polar polymer, the material is poled by applying a strong electric field (E_p)

at an elevated temperature ($T_p \geq T_g$). This introduces both induced polarization and orientational polarization via dipole alignment with the applied electric field. The temperature is then lowered below T_g in the presence of the field to freeze in the polarized state. When the electric field is removed, the induced polarization is lost but the orientational polarization remains. This preferential alignment of dipoles yields the remnant polarization, P_r, given by:

$$P_r = \epsilon_0 \Delta\epsilon E_p \tag{1}$$

where ϵ_0 is the permittivity of free space, and $\Delta\epsilon$ is the dielectric relaxation strength at T_g. For amorphous polymers, there is a linear relationship between $\Delta\epsilon$ and the piezoelectric response [1,2]

$$d_h = -(\beta/3)\epsilon_\infty P_r = -(\beta/3)\Delta\epsilon\epsilon_0\epsilon_\infty E_p \tag{2}$$

where d_h is the hydrostatic piezoelectric strain constant, β is the volume compressibility and ϵ_∞ is the dielectric constant at high frequency. To design amorphous polymers with large piezoelectric activity, P_r, β and $\Delta\epsilon$ should be maximized [2]. A molecular model has been developed which emulates the poling process in amorphous polymers and allows the calculation of P_r and $\Delta\epsilon$.

This paper presents a method of accurately predicting the orientational polarization and relaxation strength of amorphous polymers given their chemical structure. The
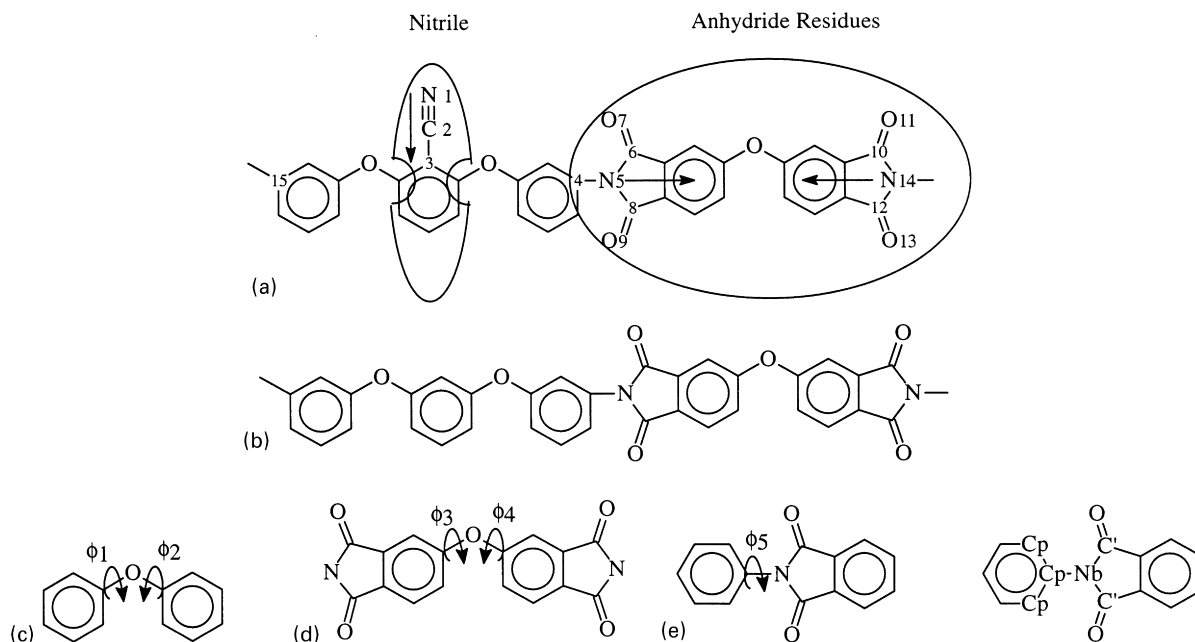
* Corresponding author.

Fig. 1. (a)Chemical structure of (β-CN) APB–ODPA showing the important polar segments, polymer dipoles and the atomic numbering scheme. (b) Chemical structure of APB–ODPA. (c) Torsional rotations studied in diphenylether. (d) Torsional rotations studied in 4,4″-oxydiphthalimide. (e) Torsional rotation studied in NPP and atom potential types.

statistical theory of orientational polarization was developed by Debye [4] and later improved upon by Onsager, Kirkwood and Frohlich [5–7], respectively. Mopsik and Broadhurst have applied these theories of polarization to piezoelectric polymers [8,9]. These theories have been successfully applied to the gas phase where the underlying assumptions are valid. When applied to the condensed phase, experimental data have been used to account for complex molecular interactions which the statistical theory is unable to accurately capture. The assumptions of the theories and the need for experimental data limits the reliability and applicability of these statistical methods. The fully atomistic model presented in this paper predicts the orientational polarization of amorphous polymers as a function of their chemical structure.

In addition to PVDF, the nitrile substituted polymer poly (vinylidene cyanide-*co*-vinyl acetate) (VDCN–VAc) [3,10] has received much attention with regard to its piezoelectric properties. Two features of the nitrile group make it advantageous for use in piezoelectric polymers. The nitrile group can easily be incorporated in many organic polymers and its large dipole moment (4.18 D) provides a strong interaction with the applied electric field. This paper focuses on the 4,4′ oxydiphthalic anhydride (ODPA) dianhydride and bis-aminophenoxybenzene (APB) diamine based polyimides. Of specific interest are the nitrile substituted (β-CN) APB–ODPA and the unsubstituted APB–ODPA polymers (Fig. 1). These polyimides are amorphous with high glass transition temperatures of 496 K and 458 K, respectively. Currently, their piezoelectric responses are an order of magnitude lower than that required for device applications [11].

Molecular modeling has been used to study the mechanisms of their response and to suggest compositional changes which might increase their response.

2. Methods

Quantum mechanical calculations were used to accurately characterize both the (β-CN) APB–ODPA and the APB–ODPA monomers. Semi-empiricial molecular orbital calculations were made using MOPAC [12] with the AM1 Hamiltonian [13,14] except where noted below. Calculations on model segments of the polymer were done to obtain information about the potential energy surfaces and the electron distributions of the segments. The torsional barriers were of particular interest because they determine the orientation of the dipoles by dictating the flexibility of the polymer backbone. The potential energy surfaces were then used to modify a force field for use in molecular dynamics simulations. The ability of semi-empirical methods to correctly assign the electronic distribution and hence dipole moments of the model segments was also examined.

Molecular dynamics simulations were used to examine the poling process. A modified CFF91 [15,16] force field was used to represent the potential energy surface of the polyimide. The intramolecular forces in the CFF91 force field were described by a quartic polynomial for bond stretching and angle bending and a three term Fourier expansion for torsional rotations. The non-bonded interactions were described by Coulombic terms and an inverse 9th power term for the repulsive and an inverse 6th power term

Table 1
The geometry of the minimum energy conformation of NPP

	6-31G[a]	6-31G**[a]	Experiment (X-ray)[a]	Modified CFF91
Torsion angle (°)	59.2	59.2	58.3	56.2
C≡N bond (A)	1.428	1.427	1.439	1.420
C=O bond (A)	1.212	1.186	1.200	1.220
C–N–C angle (°)	111.5	112.0	112.4	109.8

[a]From Ref. [20]

for the attractive van der Waals interactions. Cross terms up to the third order were also included for accuracy. The dielectric constant was set at its vacuum value of 1.0. The velocity Verlet integrator with a 1 fs time step was used to integrate the equations of motion. Non-bonded contributions to the potential energy of the system were calculated using group based cutoffs. This requires parsing the polymer chain into charge neutral groups. Non-bonded forces were calculated only if two groups were within the specified cutoff distance of each other. This avoids splitting dipoles which would introduce large errors due to erroneous monopole–monopole interactions. Because the van der Waals interactions diminish as $1/r^6$, a cutoff of 9.5 Å was used. The Coulombic forces vary as $1/r$ and a cutoff of 17.5 Å was used to allow full interaction of the polymer with the electric field while minimizing the operation count.

3. Results

3.1. Force field

Fig. 1c shows the torsional barriers of interest in the diphenylether segment of the polyimide. The potential energy surface of diphenylether was computed by rotating about φ_1 and φ_2 in 15° increments while allowing the remainder of the molecule to relax. The potential energy contours obtained by the CFF91 force field are within (1 kcal mol^{-1} of those obtained by MOPAC. Both surfaces showed broad areas of low energy characterized by transitional energies of less than 1 kcal mol^{-1}. The position of the potential energy minimum was examined by allowing the molecule to fully relax. AM1 places the energy minimum at $\varphi_1 = 40°$ and $\varphi_2 = 41°$ while the CFF91 force field places the energy minimum at $\varphi_1 = 39$ and $\varphi_2 = 39$. These results are in good agreement with ab initio results [17] and experimental data from gas phase electron diffraction [18] and X-ray diffraction [19].

The additional steric interactions in 4, 4′-oxydiphthalimide (Fig. 1d) have little effect on the potential energy surface. Like that of diphenylether, the potential energy surface is characterized by shallow minima separated by small transition barriers of about 1 kcal mol^{-1}. There is significant torsional flexibility along the backbone of these polyimides to allow the alignment of the dipoles with the electric field.

The potential energy as a function of torsion φ_5 of *N*-phenyl phthalimide (NPP) was also examined (Fig. 1e).

MOPAC with the AM1 Hamiltonian places the torsional energy minimum at $\varphi_5 = 30°$ while both experimental and ab initio methods place it at $\varphi_5 = 60°$ as indicated in Table 1 [20]. AM1 apparently does not properly account for the two competing effects which determine the potential energy minimum, the resonance interaction between the π systems of the phenyl and phthalimide rings, and the repulsive steric interaction between the carbonyl oxygen and the hydrogen on the phenyl ring.

Both the position of the energy minimum and the shape of the potential energy curve are important. Due to the shortcomings of MOPAC, the 6-31G** ab initio potential energy curve obtained by Kendric [20] was taken to be the reference curve. The native CFF91 force field incorrectly places the energy minimum at $\varphi_5 = 15°$. The force field was modified by the addition of the following parameters to reproduce the ab initio results. The carbon–nitrogen bond stretching in NPP, Fig. 1e, was described by a quartic polynomial with the following constants:

$$Cp - Nb : b_0 = 1.3912, \ K_1 = 447.044,$$
$$K_2 = -784.535, \ K3 = 886.1617$$

The NPP torsion was described by a three term Fourier expansion having the following constants:

$$C' - Nb - Cp - Cp : V_1 = -0.1047, \ V_2 = 0.2465,$$
$$V_3 = -0.0234, \ \phi = 0$$

As shown in Tables 1 and 2, the CFF91 force field thus modified gives good agreement with both experimental and ab initio results.

The interaction of the applied electric field with the molecular dipoles yields the orientational polarization underlying the piezoelectric response. Therefore, it is essential that the atomic charges which comprise the dipole moments be accurately assigned. Except for the nitrile group, the AM1 Hamiltonian was found to reproduce the dipole moments which appear in the polyimides to within 10% of the experimental values (Table 3). The inability of

Table 2
Relative energies (kcal mol^{-1}) of NPP

Torsion angle	6-31G[a]	6-31G**[a]	Modified CGG91
0°	3.2	3.9	5.2
90°	0.3	0.4	0.3

[a]From Ref. [20]

Table 3
Comparison of experimental and computed dipole moments

	Experimental dipole (D)[a]	Calculated dipole (D)	Error (%)
N-phenyl phthalimide	2.34	2.50	6
Diphenylether	1.30	1.17	10
Benzonitrile (AM1 charges)	4.18	2.71	36
Benzonitrile (PM3 charges)	4.18	4.23	1

[a] Ref. [21]

AM1 to handle the lone pair on the nitrile group leads to its erroneous calculation of the dipole moment and charge distribution (compared to ab initio results) on the nitrile atoms (N1 = − 0.021 e⁻, C2 = − 0.072 e⁻, C3 = − 0.033 e⁻). The PM3 Hamiltonian was able to reproduce the correct dipole moment of benzonitrile, and the PM3 charge distribution (N1 = −0.28 e⁻, C2 = 0.11 e⁻, C3 = 0.17 e⁻) was in good agreement with ab initio results [22]. Except for the nitrile substituent, where PM3 charges were used, the partial charges obtained from AM1 were applied to the polyimide. Table 4 shows the charges which form the important dipoles along polymer chain.

3.2. Molecular dynamics

The bulk amorphous polyimide was modelled by building an amorphous cell and applying periodic boundary conditions. An electric field was then placed across the cell and molecular dynamics was run to simulate the poling process. Once the poling was completed, P_r and $\Delta\epsilon$ were calculated. It is these parameters which control the dielectric contribution to the piezoelectric behaviour in amorphous polymers.

Modeling of the poling and analysis of the piezoelectric properties was done using the BIOSYM molecular modeling package [15]. A five unit long polymer was built and

Table 4
Partial charges of atoms. Numbering is shown in Fig. 1

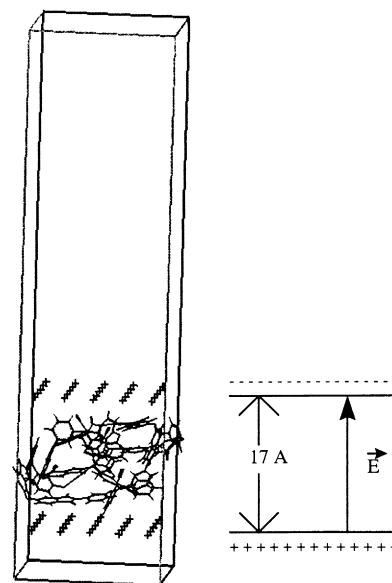| Atom number	Partial charge
1 (N)	-0.280
2 (C)	+ 0.110
3 (C)	+ 0.170
4 (C)	+ 0.086
5 (N)	-0.262
6 (C)	+ 0.361
7 (O)	-0.273
8 (C)	+ 0.363
9 (O)	-0.275
10 (C)	+ 0.361
11 (O)	-0.273
12 (C)	+ 0.363
13 (O)	-0.275
14 (N)	-0.262
15 (C)	+ 0.086

Fig. 2. The amorphous cell of polyimide with periodic boundary conditions and electric field.

packed into a cell with three dimensional periodic boundary conditions. The method of Theodorou and Suter was used to pack the chain into the cell [23]. This hybrid scheme introduces long range interactions into the RIS–Monte Carlo method of bond placement. The resultant system is of uniform density and statistically correct chain conformations. Since the polyimide systems are highly aromatic, the initial boxes were built at a low density to avoid ring catenation. Constant pressure molecular dynamics was then used to achieve an amorphous cell of experimental density, 1.34 g cm⁻³. During the constant pressure dynamics the polymer was not allowed to cross the *x*–*y* plane of the cell. This allowed the application of two sheets of stationary dummy atoms to opposite *x*–*y* faces of the cell. Equal but opposite partial charges were placed on these atoms to simulate the electric poling field. The use of three dimensional periodic boundary conditions necessitated the extension of the cell dimensions to 18.32 Å × 18.32 Å × 70 Å (Fig. 2). This eliminates the calculation of non-bonded interactions between image cells in the *z* direction. The thickness of polyimide filled portion of the cell is of the order of the persistence length of such polymers [24]. Three boxes were built and poled in the manner described previously.

The pair distribution function, $g(r)$, was examined to ensure that the cell packing technique described above yielded an amorphous system. $g(r)$ gives a measure of the probability that, given the presence of an atom at the origin of an arbitrary reference frame, there will be an atom located in a spherical shell of infinitesimal thickness dr at a distance r from the reference atom.

$$g(r) = (NA_r V)/(NA 4\pi r^2 dr) \qquad (3)$$

NA is the number of atoms in the system, *V* is the total volume of the system and NA_r is the number of atoms in
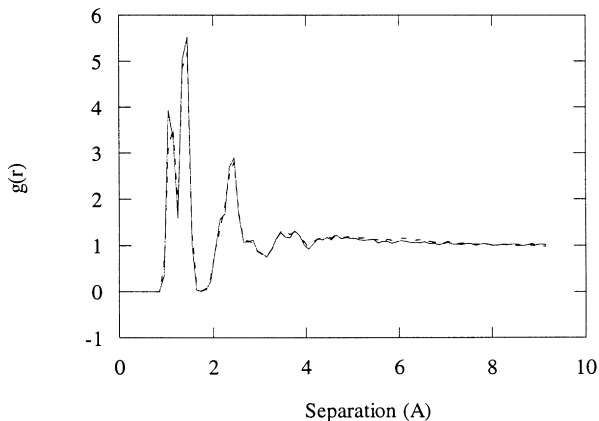
Fig. 3. The pair correlation function, $g(r)$, for both an unpoled (broken line) and poled (solid line) cell.

Fig. 4. The time evolution of the z component of the polarization after application of the electric field.

the volume element defined by r and dr. The pair distribution functions for both the unpoled and poled systems are seen in Fig. 3. The peaks at 1.05 and 1.45 Å are associated with specific atomic placements within covalent bonds, specifically the C–H bond and C–C bond, respectively. The 2.45 Å peak is due to C atoms in phenyl rings and the small hump at 3.75 Å is due to intramolecular spacings in the dianhydride. The absence of any peaks over 5.0 Å indicates that the effect of connectivity disappears at short distances. The lack of long range order shows that although the minimum cell size was used, the model system is amorphous.

The orientation of the dipoles along the polymer is governed by a Boltzmann distribution. The energy of interaction between the electric field and the dipole is given by $\mathbf{E}_p\boldsymbol{\mu}$. This interaction energy causes the population density of states to change from the equilibrium value to one which favours dipole alignment with the applied electric field. The population density is governed by

$$\text{population density} = e^{-(\mathbf{E}_p\boldsymbol{\mu}/kT_p)} \qquad (4)$$

where $\mathbf{E}_p$ is the applied electric field, $\boldsymbol{\mu}$ is the dipole moment, k is the Boltzmann constant and T_p is the poling temperature. Due to electrical breakdown within the polymer film, the experimental poling field, E_p, is of the order of $100\,\text{MV m}^{-1}$ and a poling temperature of $T_g + 5\,\text{K}$ is used. Dipole reorientation has a distribution of relaxation times depending on the viscosity of the system and the internal rotational barriers of the polymer. Under experimental conditions, the relaxation times may range from microseconds to tens of seconds [2]. The time scales of current molecular dynamics simulations are typically limited to picoseconds. It is therefore necessary to bring the experimental relaxation time into the range of times that may be explored using molecular dynamics. Assuming the experimental relaxation time to be in the microsecond range, an Arrhenius time–temperature relationship was used to determine the temperature necessary to bring the relaxation into the picosecond
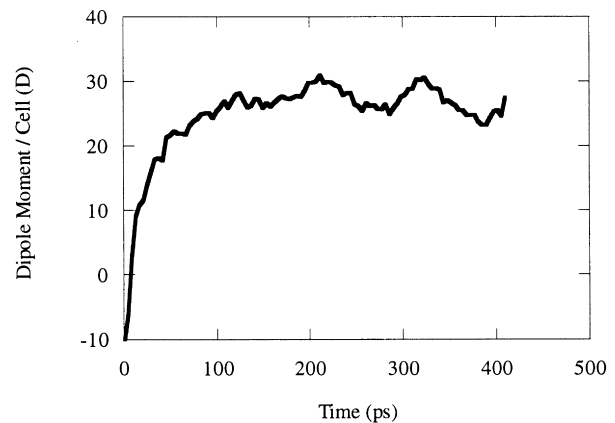
range [25]:

$$t = \hbar/kT\exp(\Delta F/kT) \qquad (5)$$

$\hbar$ is Plank's constant, ΔF is the activation free energy of the process (barrier height). Translation of the experimental values of $t = 1\,\mu\text{s}$ at $T_p = 496\,\text{K}$ requires a simulation poling temperature of 2000 K to achieve a relaxation time of 10 ps. During poling, the population density of dipoles given by Eq. (3), must be maintained at the simulation temperature. Therefore simulation of an experimental electric field of $150\,\text{MV m}^{-1}$ field applied at 496 K requires a $700\,\text{MV m}^{-1}$ field at the simulation temperature of 2000 K to induce the same level of orientation. Partial charges of $(0.055\,\text{e}^{-}/\text{atom}$ were placed on the plates of dummy atoms of the cell to simulate an applied electric field of $700\,\text{MV m}^{-1}$ in the z direction.

Molecular dynamics was run to obtain equilibrium unpoled conformations, to pole the material and finally to examine conformations in the poled state. Simulations were done on three different amorphous cells. With $E_p = 0$ (i.e. no charges on plating atoms) molecular dynamics was run at 2000 K for 50 ps. The poling field of $700\,\text{MV m}^{-1}$ was then applied at the poling temperature of 2000 K for 200 ps. The temperature was then quenched to 300 K and simulation was continued for an additional 200 ps. The durations of these simulations ensured that the model captured all of the dipole reorientation and allowed for statistically significant analysis of the data. The atomic charges and positions were used to calculate the total dipole moment of the polymer in each of the three amorphous cells during the simulation. The polarization (dipole moment per volume) was calculated by dividing the total dipole moment by the volume of the cell.

3.3. Polarization

The polarization of the cell in each of the coordinate directions was calculated as a function of time. Fig. 4 shows the polarization in the poling direction, z, after the

Table 5
Comparison of experimental and calculated values for $\Delta\epsilon$

	$\Delta\epsilon^a_{10Hz}$	$\Delta\epsilon^a_{5Hz}$	$\Delta\epsilon_{comp}$
(β-CN) APB–ODPA	11.5 ± 0.6	16 ± 1.3	17.8 ± 1.1
APB–ODPA	4.2 ± 0.5	5.7 ± 1.5	7.7 ± 1.6

electric field was turned on for one of the cells. The dipoles orient within the desired relaxation time of tens of pico-seconds. Fig. 5 demonstrates that P_r in the poling direction, z, is independent of the conformation of the starting box. In the unpoled state P_r was calculated as the average polarization during the first 50 ps of molecular dynamics when no electric field was present. On average, one would expect no net polarization. The small polarizations observed are due to the limited number of atoms being simulated and the relatively short simulation time. The poled value of P_r is the average polarization over the final 200ps of the simulation. The (β-CN) APB–ODPA polyimide had a remnant polarization of $P_r = 23.7$ mC m^{-2} (± 1.4 mC m^{-2}). Using Eq. (1), a value of $\Delta\epsilon = 17.8$ (± 1.1) was obtained. This value of $\Delta\epsilon$ agrees with the experimental values obtained by means of dielectric and thermally stimulated current techniques (see Table 5) [26]. The consistency of these results indicates that the experimental polarization of the polyimide films most likely arises from orientational polarization and not embedded charges.

The ability of pendant nitrile groups to create large polarizations has been previously demonstrated in various systems [3,27]. In (β-CN) APB–ODPA 48% of the total polarization is due to the nitrile substituent while the anhydride residues make up 39% of the total polarization (Fig. 1a and Fig. 6). These results indicate that the dianhydride portions of these polyimides play an important role not only in providing high temperature stability but also in making significant contributions to the remnant polarization and hence the piezoelectric response of the material. The addition of dipoles either as pendant groups or as part of the backbone can increase the polarization as long as backbone flexibility is maintained.

The orientational polarization can be characterized by monitoring the angles that dipoles make with the applied electric field. The projection of a dipole moment onto the
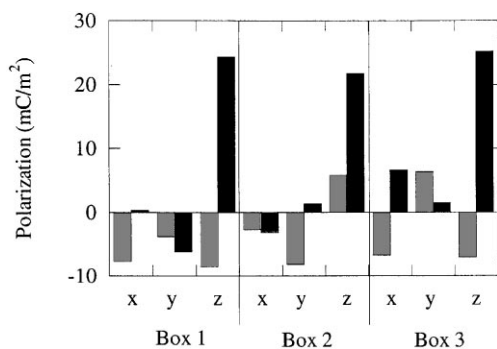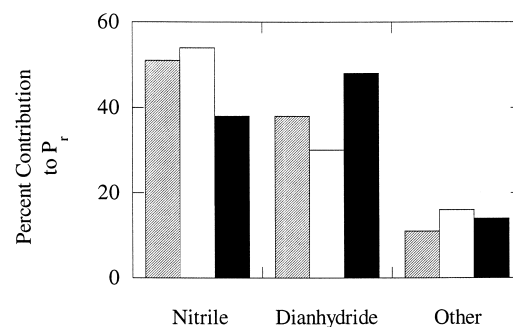

Fig. 6. The segmental contribution to the total P_r of the (β-CN) APB–ODPA system. Cell 1 (gray), cell 2 (white) and cell 3 (black).

field direction is a function of the cosine of the angle between the two. Random orientation of a vector with respect to a coordinate direction is characterized by an average angle of 90° (Fig. 7). In the unpoled state the average calculated angles between the dipoles and each of the coordinate directions are $\langle\theta_x\rangle = 97°$, $\langle\theta_y\rangle = 93°$ and $\langle\theta_z\rangle = 95°$. The fact that the average orientations are not exactly 90° explains the small polarizations in the unpoled cells, Fig. 5. This is due to both the limited size and time of the simulation. When poled the (β-CN) APB–ODPA cells show that the nitrile dipoles orient to form an average angle of $\langle\theta_z\rangle = 51°$ with the electric field while the x and y orientation remains essentially random. ($\langle\theta_x\rangle = 86°$, $\langle\theta_y\rangle = 90°$). The anhydride dipoles align to an average angle of $\langle\theta_z\rangle = 63°$ with respect to the applied electric field ($\langle\theta_x\rangle = 89°$, $\langle\theta_y\rangle = 91°$). The anhydride residue dipoles exhibit less alignment because of their smaller dipole moment and consequent weaker interaction with the electric field as well as their being part of the polyimide backbone.

For comparison and further verification of the model, unsubstituted APB–ODPA polyimide (Fig. 1b) was modelled and analysed in the same manner as (β-CN) APB–ODPA. The experimental and computational methods show that the values of $\Delta\epsilon$ are 5.7 (± 1.5) and 7.7 (± 1.6), respectively, Table 5. This 43% lower $\Delta\epsilon$ relative to (β-CN) APB–ODPA is not surprising since the previous analysis showed that 48% of the polarization was due to the nitrile substituent. Fig. 8 shows that the majority of the polarization, 83%,

Fig. 5. The components of P_r in the unpoled (gray) and poled (black) states.
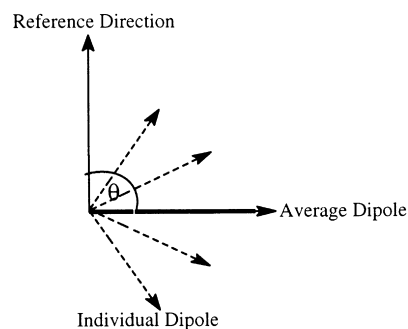

Fig. 7. Dipoles form an average angle of 90° with respect to the reference axis when randomly oriented.
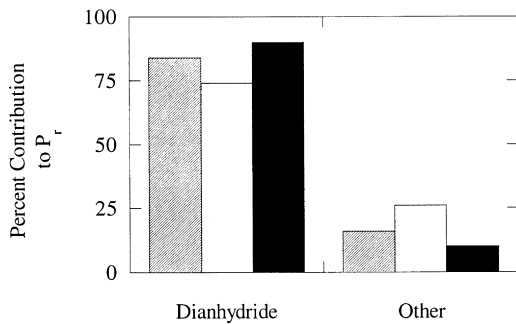
Fig. 8. The segmental contribution to the total P_r of the APB–ODPA system. Cell 1 (gray), cell 2 (white) and cell 3 (black).

is now due to the anhydride residues which on average orient to within 64° of the electric field.

Analysis shows that poling does not induce any drastic changes in the overall shape of the polyimide. The pair distribution function seen in Fig. 3 shows that the cell remains amorphous. As stated earlier, the difference between the poled and unpoled states is the average orientation of the molecular dipoles. It is the flexibility about torsional angles which allows the motion and alignment of these dipoles. Therefore, the torsional angles of the polymer were examined as a function of time and electric field. Fig. 9a and b show the probability distributions before and after poling of the two adjacent anhydride torsions (φ_3 and φ_4). In both the unpoled and poled states the conformation of the residue is $\phi_3 = 40°$ and $\phi_4 = -140°$. Yet because of the orientation of these conformations their contributions to
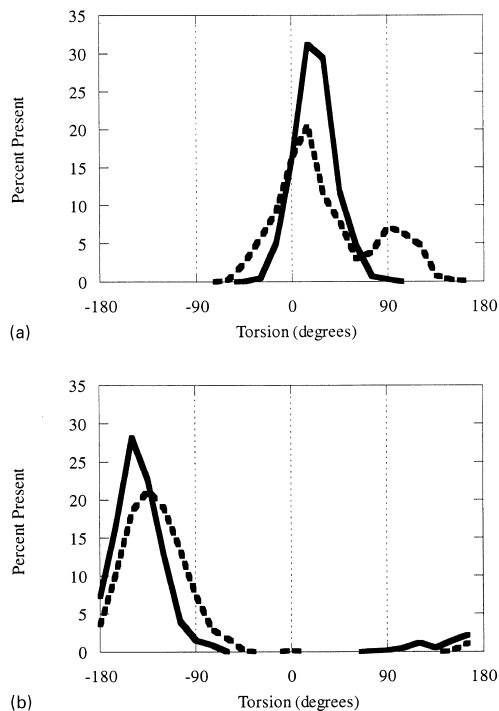

(a)

(b)

Fig. 9. (a)Torsional abundance (averaged over 50 ps) of anhydride residue torsion φ_3. Unpoled state (broken line) and poled state (solid) line. (b) Torsional abundance (averaged over 50 ps) of anhydride residue torsion φ_4. Unpoled state (broken line) and poled state (solid) line.
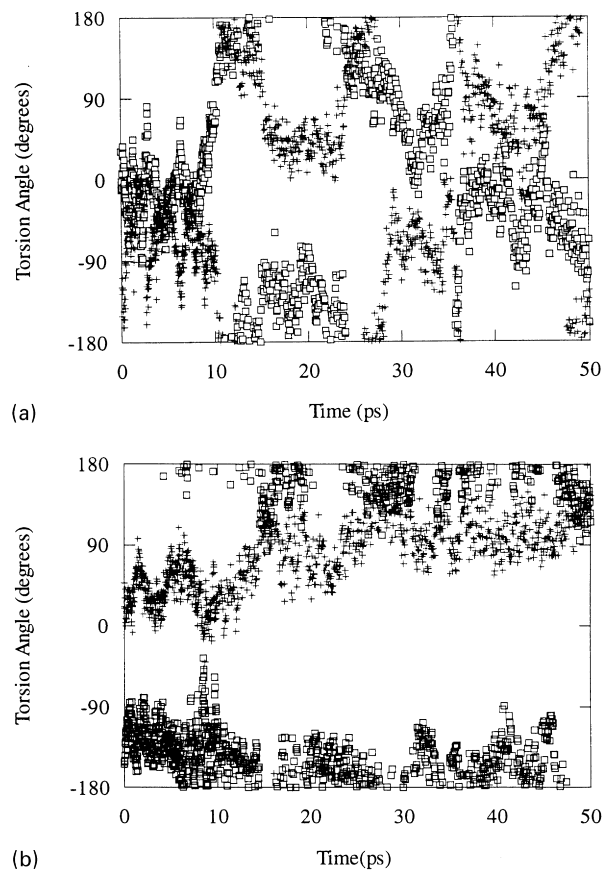

(a)

(b)

Fig. 10. (a)Evolution of ϕ_3 (+) and ϕ_4 (□) in the presence of the electric field. (b) Evolution of $\phi_3{}'$ (+) and $\phi_4{}'$ (□) in the presence of the electric field.

the polarization are − 0.30 and 2.4 D, respectively. This demonstrates that poling changes the orientation of the dipoles through overall chain motions, not individual conformational transitions. Note that the modified CFF91 force field gives reliable statistics for this torsion by placing the most populated states at approximately 40°.

Careful analysis reveals that there is no single motion responsible for the polarization of the polymer. Because the system is amorphous the interaction of a dipole and the electric field is uniquely due to the orientation of the dipole in space and its local environment. The electric field simply biases the polymer motions (i.e. torsional transitions and torsional librations) to give an average bulk polarization in the z direction. Fig. 10a shows the time evolution of two adjacent torsions within a dianhydride residue, ϕ_3 and ϕ_4, immediately after application of the electric field. Clearly, this segment undergoes conformational changes during this period which are accomplished by specific torsional transitions. Fig. 10b shows the evolution of two other chemically similar torsions upon application of the electric field. In this case the electric field simply acts to bias small torsional motions, coupled librational motion [28], which occur during poling. $\phi_3{}'$ oscillates about 180° while $\phi_4{}'$ slowly drifts from 0° to 90°. As pointed out by Moe and Ediger, this

Table 6
Parameters for free dipole rotation

	N ($\times 10^{27}$ m^{-3})	μ ($\times 10^{-29}$) cm	$\epsilon(0)$	n	$\Delta\epsilon_{free}$
(βCN) APB–ODPA	1.36	2.95	20.00	1.67	23.06
APB–ODPA	1.42	1.56	8.65	1.68	6.86

motion may allow a vector to reorient by 30°. This is of the order of the reorientation experienced by the nitrile and anhydride residue dipoles. The electric field biases both conformational transitions and small librational motions to yield time averaged polar polymer conformations. Similar conclusions were reached about the torsional changes which dictate the nitrile orientation since the orientation of each nitrile dipole is unique.

Additional information about the piezoelectric behaviour associated with orientational polarization can be gained by comparing the results with dielectric theory of the expected dielectric relaxation, $\Delta\epsilon_{free}$, due to free (i.e. uncorrelated) rotation of the dipoles[7].

$$\Delta\epsilon_{free} = (N\mu^2/3kT\epsilon_0)(n^2 + 2/3)2(3\epsilon(0)/2\epsilon(0) + n^2)^2 \qquad (6)$$

N is the number density of dipoles, μ is the dipole moment per unit, k is the Boltzmann constant, $\epsilon(0)$ is the static dielectric constant and n is the refractive index. Large dielectric relaxations of up to four times $\Delta\epsilon_{free}$ are seen in the nitrile substituted copolymer PVDCN–VAc [29]. This is attributed to the cooperative motion of polymer segments consisting of up to four monomer units. The development of polymers with large dielectric relaxations is one of the most effective ways of increasing the piezoelectric properties (see Eqs. (1) and (2)). Eq. (6) was used to examine the possibility of cooperative motion of the dipoles in the polyimides. Using the values shown in Table 6 and taking the dipole moment of the reorienting unit to consist of contributions from the nitrile group and the two NPP groups, values of $\Delta\epsilon_{free} = 23.06$ and $\Delta\epsilon_{free} = 6.86$ were obtained for the (β-CN) APB–ODPA and APB–ODPA polymer, respectively. These results are in good agreement with both the experimentally observed and computationally obtained values of $\Delta\epsilon$. The molecular dipoles of both (β-CN) APB–ODPA and APB–ODPA can be regarded as undergoing free rotational motion, therefore, no cooperative motion is indicated.

4. Conclusion

A model has been developed which accounts for the dielectric relaxation strengths of polyimides in terms of their chemical structure. A method of constructing a model of an electroded amorphous polymer film has been presented. This required the use periodic boundary conditions to simulate the bulk material and the use of plating atoms by which to apply the electric field. Molecular dynamics simulations were run using elevated temperatures

and electric fields to reduce the time scale of the polarization process. From this model, dielectric relaxation strengths were calculated which are in excellent agreement with experimental results. The values of $\Delta\epsilon$ for two polyimides were then explained in terms of their chemical structure. This model can form a basis for the development of amorphous polymers with increased piezoelectric responses.

References

[1] Furukawa T. IEEE Trans Electr Insulation 1989;24 (3):375.
[2] Davis GT. In: Wong CP, editor. Polymers for electronic and photonic applications. Boston, MA: Academic Press, 1993.
[3] Nalwa HS. Ferroelectric polymers. New York: Marcel Dekker, 1995.
[4] Debey P. Phys Z 1912;13:97.
[5] Onsager L. J Am Chem Soc 1936;58:1486.
[6] Kirkwood JG. J Chem Phys 1939;7:911.
[7] Frohlick H. Theory of dielectrics. New York: Oxford University Press, 1958.
[8] Broadhurst MB, Davis GT, McKinney JE, Collins RE. J Appl Phys 1978;49(10):4992.
[9] Mopsik FI, Broadhurst MG. J Appl Phys 1975;46 (10):4204.
[10] Tasaka S, Inagaki N, Okutani T, Miyata S. Polymer 1989;30:1639.
[11] Simpson J, Ounaies Z, Fay C. In: George EP, Gotthardt R, Otsuka K, Trolier-McKinstry S, Wun-Fogle M, editors. Materials Research Society Proceedings: materials for smart systems II, vol. 459. Pittsburgh, PA: Materials Research Society, 1997.
[12] Stewart JJP. MOPAC, QCPE Program number 455.
[13] Zerner MC. In: Lipkowitz KB, Boyd DB, editors. Reviews in computational chemistry II. New York: VCH, 1991:346.
[14] Dewar MJS. J Am Chem Soc 1985;107:3902.
[15] BIOSYM Molecular Modeling Software: Version 4.0.0, Molecular Simulations, Incorporated, September 1996.
[16] Maple JR, Hwang MJ, Stockfisch TP, Dinur U, Wlkdman M, Ewig S, Hagler AT. J Comput Chem 1994;15:162.
[17] Jaffe RL. Polymer preprints, American Chemical Society, Division Polymer Chemistry 1989;30:1.
[18] Naumov VA, Ziatdinova RN. Z Struct Khim 1984;25:88.
[19] Boon J, Margre EP. Makromol Chem 1969;126:130.
[20] Kendrick J, Robson E, McIntyre S. J Comput Chem 1992;13(4): 408.
[21] Lide D, editor. CRC handbook of chemistry and physics 75th edition. Ann Arbor, MI: CRC Press, 1994:9–45.
[22] Dimitrova Y. Theo Chem 1996;362:23.

[23] Theodorou DN, Suter UW. Macromolecules 1985;18(7):1467.

[24] Zhang R, Mattice WL Marcomolecules 1993;26:6100.

[25] Chelkowski A. Dielectric physics. New York: Elsevier, 1980.

[26] Ounaies Z, Young J, Simpson J, Farmer B. In: George EP, Gotthardt R, Otsuka K, Trolier-McKinstry S, Wun-Fogle M, editors. Materials Research Society Proceedings: materials for smart systems II, vol. 459. Pittsburgh, PA: Materials Research Society, 1997.

[27] Tasaka S, Toyama T, Inagaki N Jpn J Appl Phys 1994;33:5838.

[28] Moe NE, Ediger MD Macromolecules 1996;29:5484.

[29] Furukawa T, Munehiro D, Nakajima K, Kosaka T, Seo I Jpn J Appl Phys 1986;25 (8):1178.